

Interannual Variability of Rainfall over the West Africa Sahel

Aichetou Dia-Diop¹, Sinclair Zebaze², Malick Wade¹, Rinelle Ngongang Djiondo², Bouya Diop¹, Eric Efon³, Andre Lenouo^{2*}

¹Laboratoire des Sciences de l'Atmosphère et des Océans-Matériaux-Énergie-Dispositifs (LSAO-MED), Université Gaston Berger, Saint-Louis, Sénégal

²Department of Physics, Faculty of Science, University of Douala, Douala, Cameroon

³Department of Physics, Faculty of Science, University of Bamenda, Bamenda, Cameroon

Email: *lenouo@yahoo.fr

How to cite this paper: Dia-Diop, A., Zebaze, S., Wade, M., Djiondo, R. N., Diop, B., Efon, E., & Lenouo, A. (2020). Interannual Variability of Rainfall over the West Africa Sahel. *Journal of Geoscience and Environment Protection*, 8, 85-101.
<https://doi.org/10.4236/gep.2020.83007>

Received: February 8, 2020

Accepted: March 28, 2020

Published: March 31, 2020

Copyright © 2020 by author(s) and Scientific Research Publishing Inc. This work is licensed under the Creative Commons Attribution International License (CC BY 4.0).

<http://creativecommons.org/licenses/by/4.0/>



Open Access

Abstract

Interannual variability of the precipitation over West Africa Sahel is analyzed based on 32 years (1979-2010) from monthly and daily database of the Global Precipitation Climatology Project (GPCP). In this region, we found that there is a link between the West Africa Monsoon (WAM) and the daily means of the precipitation in the summer, unseasonal rains can occur in the transition seasons and even in the heart of the dry season. Rainfall is the most important element for agro-pastoral activities in this region. The 850-hPa wind and wind divergence structure show a maximum convection over Mountain region (Fouta-Djalou and Mont-Cameroon) which corresponds to the high precipitation and OLR observed in these regions. The trend and empirical orthogonal function (EOF) of the precipitation are presented, including the mid-July variability of the precipitation. The dominant EOF of GPCP precipitation accounts for around 25.3% of the variance with slightly large amplitude in the north while relatively small in the equatorial band respectively. The second and third EOF which accounts for 20.5% and 14%, describes a longitudinal contrast with a zonal gradient.

Keywords

GPCP Precipitation, West Africa Monsoon, Inter Tropical Convergence Zone, Trend

1. Introduction

Sahel is an area of semi-arid expanse of grassland, shrubs and small thorny trees found in Southern Sahara Desert (Nicholson, 2013). This region extends about

5000 km across Africa from east to west and from the Sahara to the humid savannah at roughly 10°N, even though more precisely, “Sahel” applies to a smaller region between latitudes 14°N and 18°N. Sahel includes the countries like Sudan, Chad, Mali, Senegal, Niger, Mauritania, Burkina Faso (northern part), Nigeria (northern part). Most of the local population in this region live in rural areas and practise agriculture. Hence, variabilities of climatic parameters are of great importance to the region.

Scientific investigations were focused on the Sahel in the 1970s, 1980s and 2000s because of the long period of drought that had ravaged the region and the effects of desertification. Recently, Sahel has again received much meteorological attention as many field experiments have been carried out in order to better understand climatic variabilities in the region. These experiments include the AMMA (African monsoon multidisciplinary analysis) experiment, that took place in 2006 (Redelsperger et al., 2006; Janicot et al., 2008), the associated Model Intercomparison Project (ALMIP, Boone et al., 2009), the AMMA Catch Experiment (Lebel et al., 2009), which extended AMMA into the region of Benin, and the JET2000 Experiment, that focused on the African Easterly Jet (Thornicroft et al., 2003).

These experiments show that in Sahel, summer season is dominated by the West African Monsoon (WAM). Many atmospheric features, such as monsoon flow, African Easterly Jet (AEJ), Tropical Easterly Jet (TEJ), African Easterly Waves (AEWs) and Mesoscale Convective Systems (MCS) characterize the WAM. Rainfall over the Sahel depends on the northward inland propagation of the rain band associated to the Intertropical Convergence Zone (ITCZ). This makes the Sahel rainfall subject to high variability such as intraseasonal, inter-annual and interdecadal (Diallo et al., 2012; Lenouo et al., 2016). To understand the origin of this variability, several mechanisms have been identified such as Sea Surface Temperature (SST) anomalies (Fontaine et al., 1995; Giannini et al., 2003; Hoerling et al., 2006; Nicholson & Webster, 2007; Hagos & Cook, 2007) continental surface conditions (Semazzi & Sun, 1997; Wang & Eltahir, 2000) and atmospheric structures (Nicholson & Grist, 2001; Jenkins et al., 2010; Nicholson, 2008), in addition to a possible effect of the global climate change (Paeth & Hense, 2004). Besides, the dynamics of the low-level monsoon flow over West Africa, the mid-tropospheric AEJ and the upper-level TEJ in modulating the rainfall variability at both intraseasonal and interannual timescales is an established result (Le Barbé et al., 2002; Lenouo et al., 2005; Nicholson, 2013).

Several studies link variability in general circulation features and atmospheric moisture transport anomalies to sub-Saharan rainfall. Correlated monthly vertical motion patterns and rainfall over Africa from 1951 to 1975 for January, April, July and October exceed 95% confidence over most areas affected by seasonally migrating rainbelt (Kidson, 1977). Correlations were “barely significant” and vertical motion data were not sufficient to indicate relationships between rainfall departures and departures from seasonal vertical motion when the annual cycle

was removed (Kidson, 1977).

Northern Hemisphere circulation shifts and weakening have been linked to anomalously low Sahelian rainfall to weakening. Weakening in Sahel region appears as near disappearance of the 850-mb trough (Kidson, 1977), a weakened TEJ (Newell & Kidson, 1984; Fontaine et al., 1995), and a decrease in southwesterly monsoonal flow (Fontaine & Janicot, 1992). Some studies have examined drought during years 1967 and 1968 (Lamb, 1978) and years 1953-63 and 1968-75 (Fontaine & Janicot, 1992) and showed that it corresponded to a southward displacement of the ITCZ. On the other hand, some studies covering different time periods haven't detected a systematic southward movement of the ITCZ. These studies can be found in Newell and Kidson (1984) which analyzed data covering 1958-63 and 1969-73, or Nicholson (1981) which examined a dataset extending from 1900 to 1973. These authors found that during some wet (dry) years, the ITCZ extended northward and the Hadley cell's descending branch expanded (contracted).

Fontaine et al. (1995) showed that rainfall anomalies are related to wind behaviour in the coast of Guinea and Sahel. They found that rainfall anomalies in these regions were of opposite sign most often. In addition, the Sahel zone drought—Guinea zone flood scenarios corresponded to an increased, southward, low-level, meridional temperature gradient and a stronger wind velocity at the AEJ's southern border. This study proposes to explore the interaction between rainfall and dynamics mechanisms events at annual time scales and evaluate their modification in the climate system over West Africa Sahel in way to add the literature. Datasets and methods used are briefly described in Section 2. Section 3 investigates the characteristic of precipitation and annual cycle associated with African Easterly wave's activity. Finally, Section 4 summarizes the main results and gives some prospects for future work.

2. Data and Methodology

2.1. Data

The in-situ data are obtained from CERAAS (Centre d'Etude Regional pour l'Amélioration de l'Adaptation à la Sécheresse) which is a national laboratory of ISRA (Institut Sénégalais de Recherches Agricoles) and a regional pole of excellence in the study of drought adaptation of species cultivated in dry areas. The knowledge acquired on the agro-physiological behaviour of plants in drought conditions has been enhanced by the development of tools and methodologies for the early estimation of agricultural production. These daily precipitation data are from 1950 to 2010 at the synoptic stations of St Louis (16°27'W - 16°03'N), Louga (15°37'N - 16°13'W), Linguère (15°23'N - 15°07'W), Dagana (16°47'N - 15°6'W), Podor (16°39'N - 14°58'W) and Matam (15°39'N - 13°15'W) (Salack et al., 2016). **Figure 1** shows the evolution of the standardized rainfall index over these synoptic stations where rainfall was regular at Louga, Linguere and Matam in contrary to Saint-Louis and Podor where the dry years are dominant.

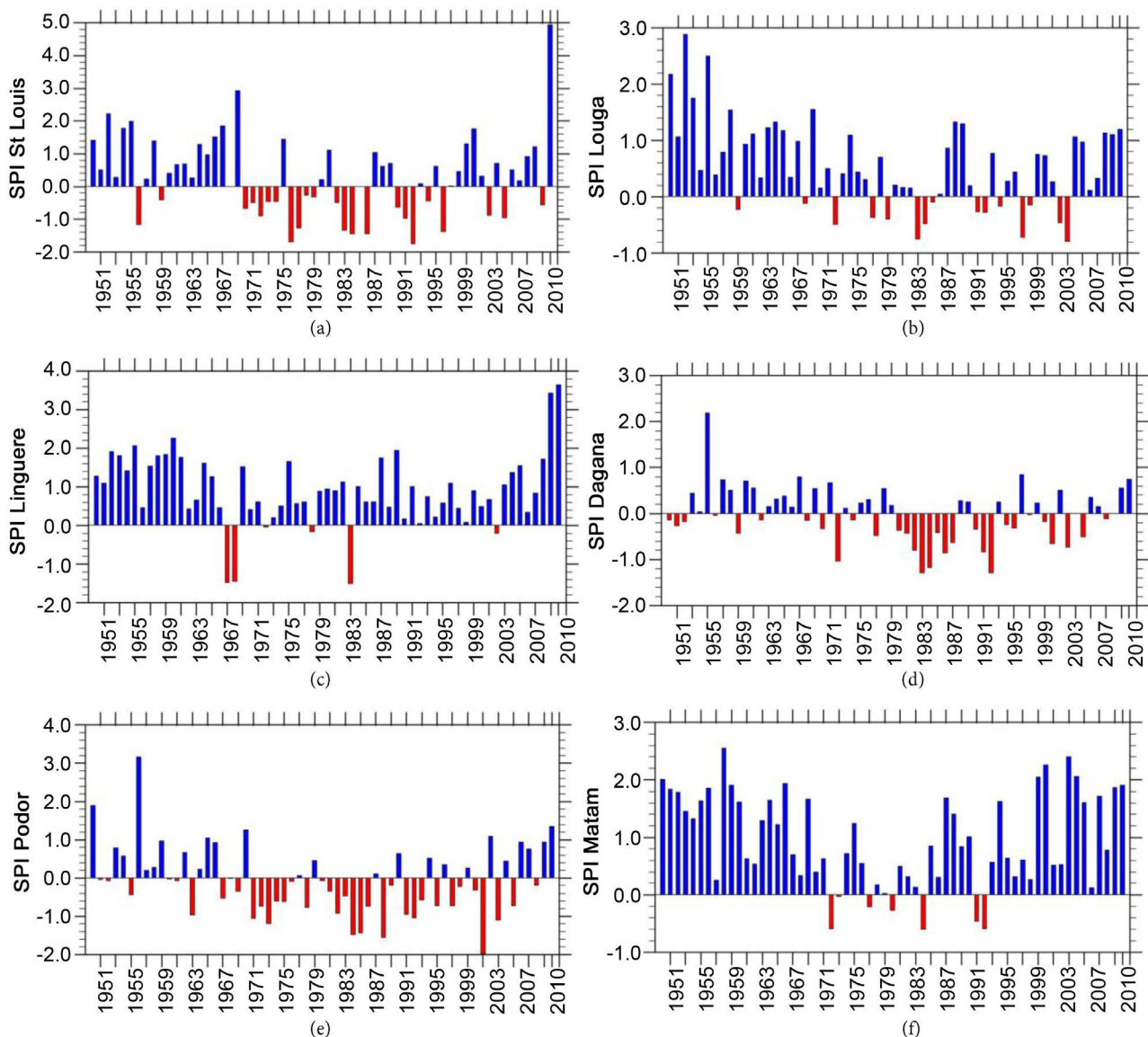


Figure 1. Evolution of the standardized rainfall index over synoptic stations in the Northern of Senegal between 1950 and 2010 at (a) St Louis ($16^{\circ}27'W - 16^{\circ}03'N$), (b) Louga ($15^{\circ}37'N - 16^{\circ}13'W$), (c) Linguère ($15^{\circ}23'N - 15^{\circ}07'W$), (d) Dagana ($16^{\circ}47'N - 15^{\circ}6'W$), (e) Podor ($16^{\circ}39'N - 14^{\circ}58'W$) and (f) Matam ($15^{\circ}39'N - 13^{\circ}15'W$). The standardized rainfall index is an average of rainfall standardized at each station with respect to the mean of the station: $R^* = (R - m)/s$ where m and s are the mean and standard deviation respectively of the rainfall series at the station.

Rainfall data are obtained from the Global Precipitation Climatology Project (GPCP) one-degree daily (1DD) version 2.2. It is combined with the precipitation dataset from polar satellite-estimated (SSM/I emission estimates) and GPCP geostationary satellite precipitation data centre (GPI and OPI estimate rain gauge). The dataset used covers the period from 1998 to 2008 (daily) and 1979 to 2010 (monthly). This product has been validated regionally and globally by McCollum et al. (2003); Dinku et al. (2007) and Ruiz et al. (2010). While the 1DD GPCP rainfall data is available over a rather short period, this product seems to be essential over Africa where topography and surface conditions force

high rain spatial variability (Thomas et al., 2009; Vondou et al., 2010; Tchakoutio et al., 2012) and where OLR values may not be always highly correlated with rainfall quantities.

We also use 6-hourly ERA-Interim data for 36 years (1979-2014) on the latitude-longitude resolution of $0.75^\circ \times 0.75^\circ$ (available at <http://data.ecmwf.int/data/>). We derived wind speed (U) and wind divergence from ERA-Interim. Vertical cross-sections extending from 1000 to 500 hPa (every 25 hPa from 1000 to 750 hPa and every 50 hPa from 750 to 500 hPa) were used to identify heat, moisture, and wind-speed gradients from 20°W to 30°E and from Equator to 30°N (Dee et al., 2011).

Most often, outgoing longwave radiation (OLR) is used to investigate AEW (Wheeler & Kiladis, 1999; Roundy, 2008; Kiladis et al., 2009; Zebaze et al., 2017). The present study uses daily OLR dataset obtained from NOAA from 1974 to the present day with a time resolution of two measurements per day and per grid point (Liebmann & Smith, 1996). The local time of passage of the satellites varied during the entire period of observation. Hence, for maximum consistency in the data sets, we have retained only the years from 1980 to 2009 for which measurements were made at 7:30 and 14:30 LST. As has already been shown in previous studies (Janicot, 2011), this provides a realistic estimate of the daily average, especially for analysing the intra-seasonal time scale.

2.2. Methodology

Nguyen and Duvel (2008) showed that strong and reproducible 5 - 6 days oscillation characterise dominant modes of boreal spring synoptic variability. Seasonal cycles were removed before calculating spectra for each month segment during 1980-2009. Spectra are calculated on each individual month and averaged over 11 years. a 3-point Daniell smoother is applied to the spectral estimates (Daniell, 1946) to maximize degree of freedom. A red noise background spectrum is computed from the formula of Gilman et al. (1963). The 95% confidence limits about this red noise spectrum are determined using F-statistic.

Wavelet analysis is a common tool for decomposing a time series into a time-frequency space and detecting time-frequency variations. Wavelet transform allows comparing a signal to a wavelet function called mother wavelet (here the Morlet wavelet is used; Torrence & Compo, 1998). After testing different mother wavelets, the results obtained look similar. Because the wavelet transform is a band pass filter with a known response function (the wavelet function), it is also a powerful filtering technique. In order to identify the dominant synoptic modes, the wavelet analysis method is, therefore, employed here over West Africa during 1980-2009 since in signal processing; wavelets are very useful for processing non-stationary signals.

2.3. Statistic Analysis

2.3.1. Empirical Orthogonal Function

Also called Principal Component Analysis (PCA), the Empirical Orthogonal

Function (EOF) is a multivariate statistical technique which consist to reduce a data set containing a large number of ($K \times 1$) data vector x to a data set containing fewer new ($M \times 1$) vectors u variables, and that are linear combinations of the original ones and which contain most of the information in the original collection of x 's. The elements of these new vectors u are called the principal components (PCs). Mostoften, the principal component is calculated by using the anomalies $x' = x - \bar{x}$. The first PC, u_1 , is that linear combination of x' having the largest variance. The subsequent principal components u_m , $m = 2, 3, 4, \dots$, are the linear combinations having the largest possible variance, subject to the condition that they are uncorrelated with the principal components having lower indices.

The m^{th} principal component of the elements u_m from u are obtained as the projection of the data vector x' onto the m^{th} eigenvector, e_m , of the covariance matrix of x , $[S]$ is given by the relation (Wilks, 2011):

$$u_m = e_m^T x' = \sum e_{k,m} x'_k, \quad m = 1, 2, \dots, M \quad (1)$$

where the transpose operation is denoted by the superscript T and each of the M eigenvectors contains one element pertaining to each of the K variables, x_k .

2.3.2. Trends

The Mann-Kendall trend test (MKTT) is a non-parametric alternative used to investigate the possible trend of a time series. In the case for example of a time series x_i (with i varying from 1 to n), the static test for the MKTT is obtained using the formula (Wilks, 2011):

$$\tau = \sum_{i=1}^{n-1} \text{sgn}(x_{i+1} - x_i) \quad (2)$$

In the case where the time series x_i decreases or increases, $\text{sgn}(x_{i+1} - x_i)$ takes the value -1 or $+1$ respectively. When the time series x_i is constant, $\text{sgn}(x_{i+1} - x_i)$ is equal to zero.

We applied the MKTT to test the presence of the trend in precipitation and to analyze the local seasonal trends in this parameter. The magnitude of the trend of precipitation is estimated by linear regression, and trends included in the analysis have their probability exceeding the 95% significance level.

3. Results and Discussion

The Climatology over West Africa

Most recent research on the intraseasonal variability of the West African monsoon's (time scale of 10 to 90 days) has centered on the Madden-Julian Oscillation (MJO). Generally, its origin is over the Pacific warm pool, from which an eastward-propagating Kelvin wave and a westward-propagating Rossby wave emanate (Zebaze et al., 2015). A similar phenomenon can also occur over the Indian Ocean providing a link between the Indian and African monsoons. Occurring in the boreal summer, these waves meet over West Africa, where they spawn convection and modulate easterly wave activity, the wind regime, and

moisture transport (Nicholson, 2013). **Figure 2** shows that the maximum rainfall effectively occurs in mid-August over West Africa.

The spatial evolution during the summer is presented in **Figure 3**. The maximum rainfall can be found in the West Africa coastal zone and particularly around the Fouta-Jalon Mountain. climatological monthly means of precipitation (1979-2014) over West Africa from GPCP reanalysis can be found in Ndao et al. (2019).

The trend of the precipitation presents a maximum at the center of Senegal in August, which corresponds to the presence of ICTZ in this region as presented in **Figure 4**. Depending on the local rainfall peak, Thorncroft et al. (2003) defined four phases of the West African monsoon: oceanic, coastal, transitional, and Sahelian. During the oceanic phase, between November and mid-April, a broad rainbelt lies just north of the equator. During the subsequent coastal phase, which generally prevails to mid-June, peak rainfall lies over the ocean but in the near-coastal region around 4° to 5° North. The transition phase, when a decrease in rainfall is observed, occurs in early July. Le Barbé et al. (2002) refer to these first three phases collectively as the oceanic regime. The Sahelian phase lasts from mid-July to September. Throughout this last phase, the rainfall peak is

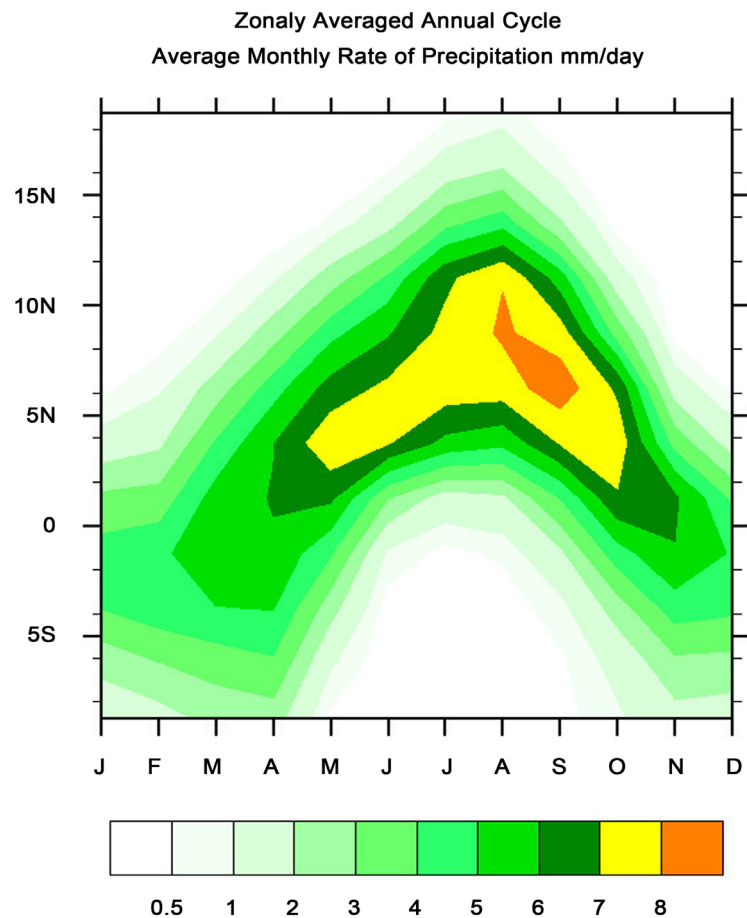


Figure 2. Time-latitude mean monthly rate of GPCP precipitation between 13°W and 17°W during the period 1979 to 2010 in mm/day.

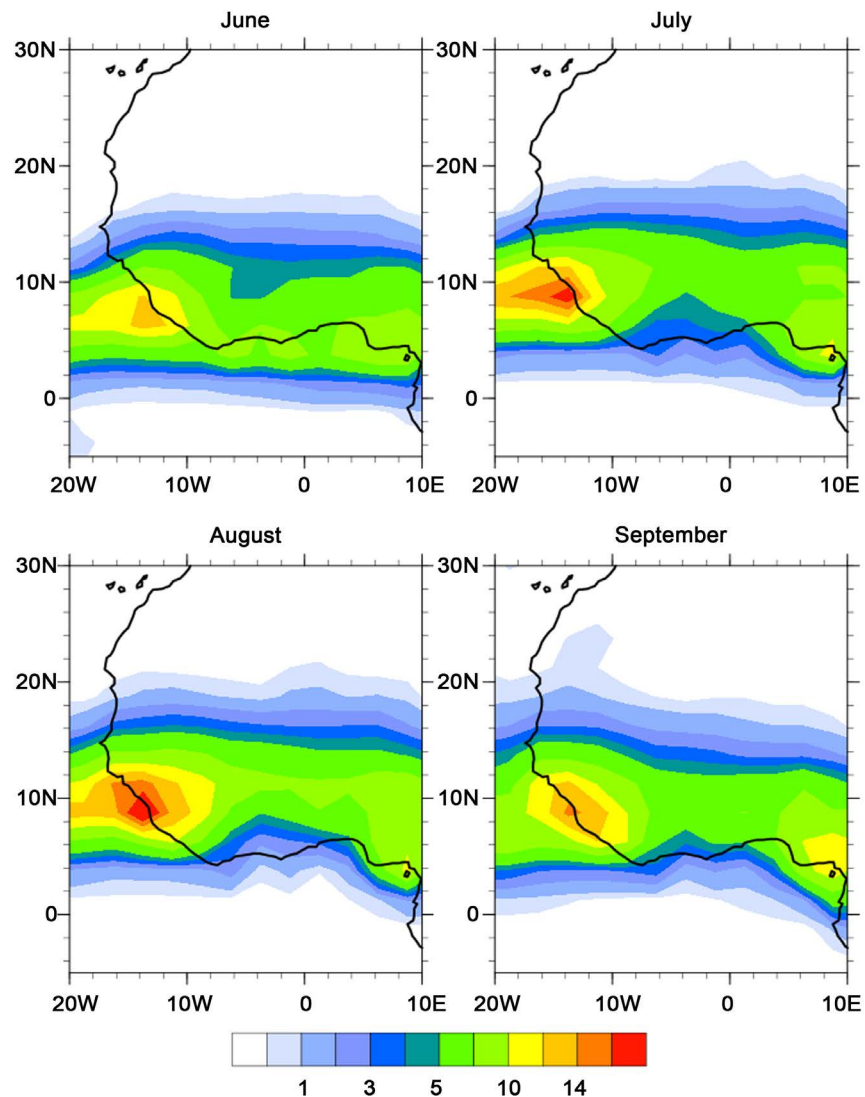


Figure 3. Daily climatology of JJAS average daily of GPCP precipitation during 1979-2008 in mm/day over West Africa.

more intense and remains just to the south of the Sahel, around 10°N. Rainfall in the Sahel zone is associated with this maximum, with [Lebel et al. \(2009\)](#) term in the continental regime.

The structure of 850 hPa wind anomalies (mean) (vectors), negative unfiltered OLR anomalies (mean) and precipitation anomalies are presented in [Figure 5](#). Convection and enhanced precipitation accompany enhanced trade winds. The 850-hPa wind and wind divergence structure show a maximum convection over Mountain regions (*i.e.* Fouta-Djalon and Mont-Cameroon) which corresponds to the high precipitation and OLR observed in these regions. Convective activity over West Africa occupies a relatively smaller area. Increase in rainfall associated with African wave activity is consistent. Recent studies suggest that convective wave initiation is favoured by the ITCZ when it is closer to the equator during these months ([Nguyen & Duvel, 2008](#); [Zebaze et al. 2017](#)). The latitude band

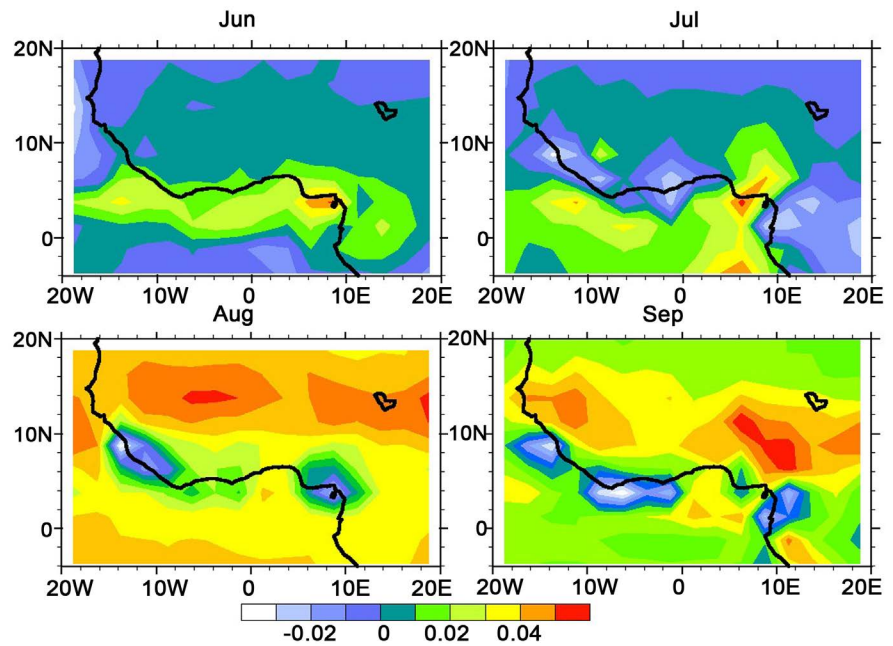


Figure 4. Trend of JJAS daily of GPCP precipitation during 1979-2008 in mm/day over West Africa.

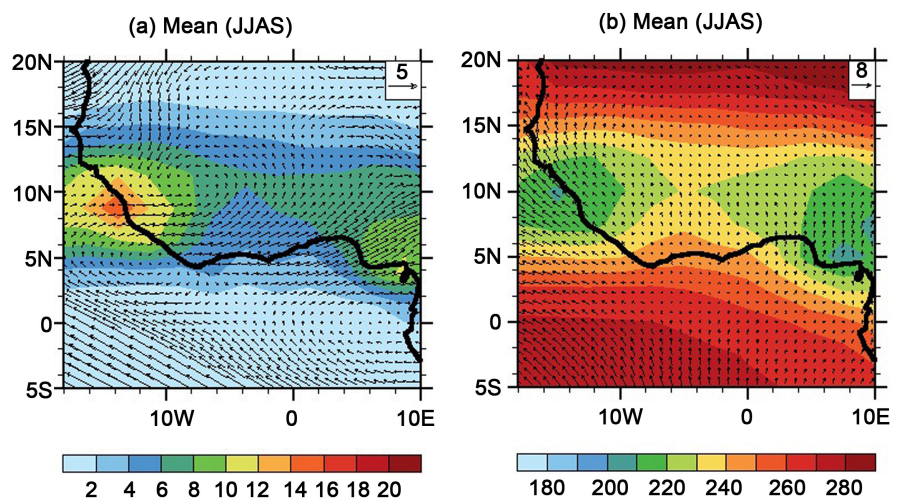


Figure 5. Graphs of (a) Mean wind at 850 hPa and GPCP precipitation (in mm/day) and (b) the divergence of wind at 850 hPa and OLR (in W/m^2) over West Africa.

of significant precipitation anomalies is slightly larger during April and June.

As mentioned earlier, previous studies show that on synoptic times-scales, precipitation over West Africa during boreal spring is dominated by variability on both 3 - 5 and 5 - 6 day times-scales. To calculate the spectra, the smoothed seasonal cycle was first removed from each time series. The data was then subdivided into the individual June-September time periods from each year. The first and last 5% of each June - September time series was tapered using a cosine bell function to reduce spurious results in the frequency response function. The spectra were found for each year, and then averaged across all of the years (11 for

GPCP). 95% confidence limits and Red noise were determined using the theoretical Markov spectrum methods. Spectral peaks that are statistically significant at the 95% confidence level will stand above the upper limit of these curves.

Over the West Africa, four main spectral peaks for precipitation exist at the synoptic time scales (**Figure 6**). One spectral peak is centred near a period of 3 days, and another peak is centred around a period of 5 days. The 3-day peak is presumably in association with African easterly waves (Reed et al., 1977; Lenouo et al., 2005) and with convective activity over land. The 5-day peak corresponds to 5 - 6 days synoptic variability found by Nguyen and Duvel (2008).

Figure 7 shows the mean wavelet spectrum averaged for the period 1980-2009 of unfiltered OLR anomalies over the Northern Senegal ($14^{\circ}\text{N} - 16.5^{\circ}\text{N}$ and $12^{\circ}\text{W} - 16.5^{\circ}\text{W}$). The largest oscillations of convection are observed in June - August with synoptic variance between 2 and 5 days. In northern winter, depending on the regions, high variances are also present. In summer, the ITCZ migrates northward and the synoptic AEW becomes the main feature of rainfall in this region. The relationship between convection and AEWs is complex. It was originally thought that they principally organize convection. Recently, research has shown feedback relationships in which convection can modulate waves, which in turn modulate convection. Nicholson (2013) suggested that the mesoscale convection systems (MCSs) that bear most of West Africa's precipitation are often imbedded in the northerly flow ahead of the wave trough. More recent work has also shown the relationship between AEWs and convection to be much more complex (Lenouo et al., 2016).

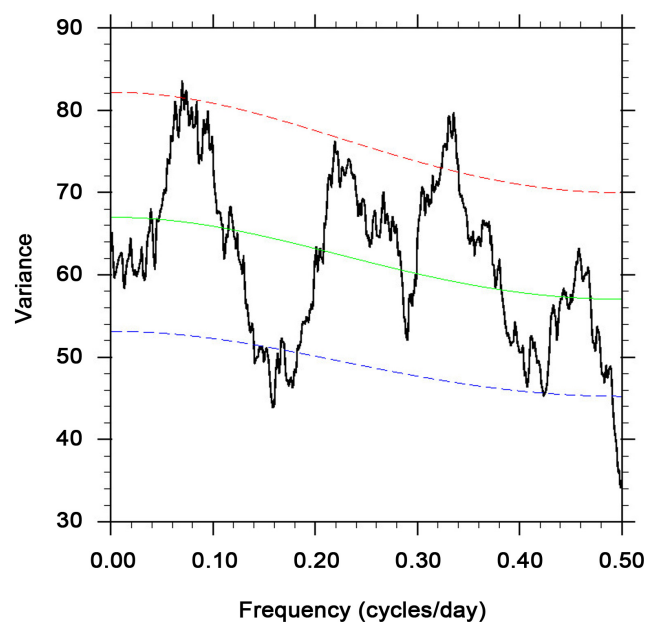


Figure 6. Power spectrum of the daily JJAS precipitation variance between $14^{\circ}\text{N} - 16.5^{\circ}\text{N}$ and $12^{\circ}\text{W} - 16.5^{\circ}\text{W}$ (Northern region of Senegal) obtained from Fast Fourier Transformation (FFT). The climatological seasonal cycle was removed before computation of the spectrum. Also shown are the red noise background spectrum and the 95% confidence limits on this background spectrum.

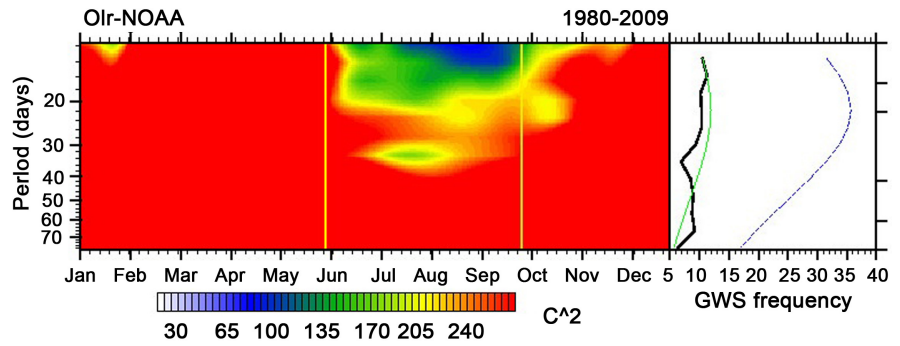


Figure 7. OLR JJAS Diagrams of the mean wavelet variance averaged over West Africa during 1980-2009 of daily unfiltered OLR anomalies. The mean seasonal cycle and inter-annual variability were removed before computing the spectrum. The green and blue lines are low and higher frequency band respectively.

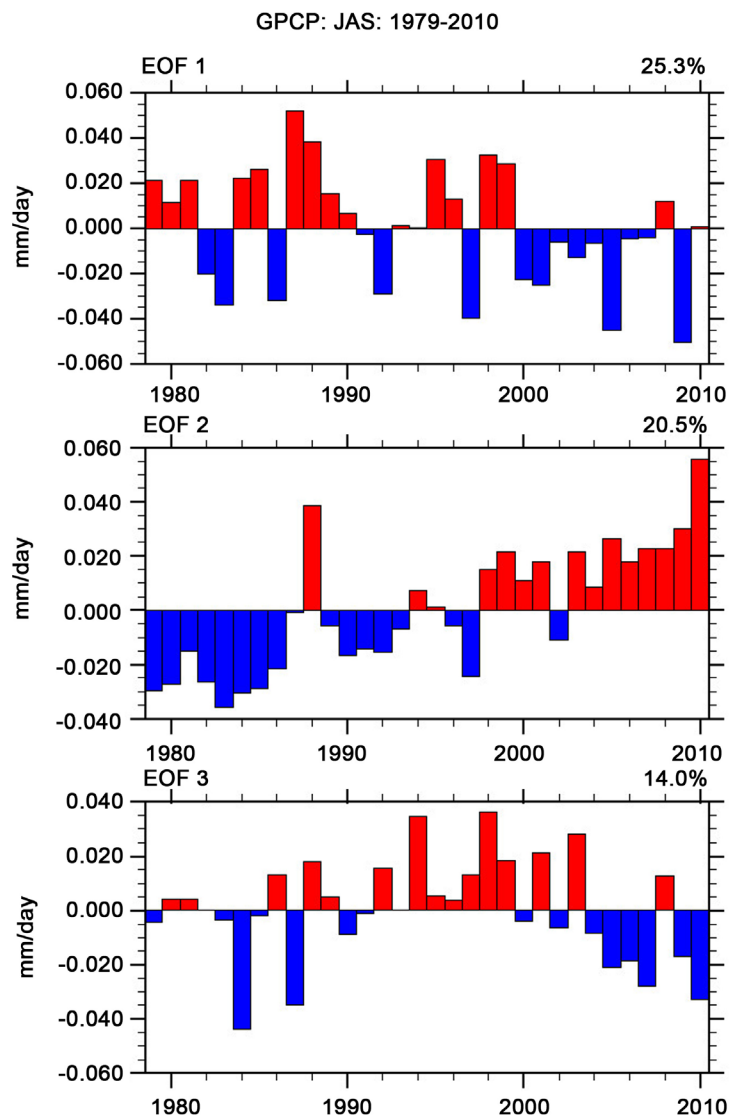


Figure 8. First three PC of GPCP precipitation over West Africa during June - July - August 1979-2010. Percentage of total variance accounting for the pattern appears on top right corner.

Figure 8 shows the first three PC of GPCP precipitations over West Africa during the summer (JAS) from 1979 to 2010. We chose the period of JAS but not JJAS because convection is more important during that period from **Figure 7**. The PC1 is in the positive phase for the years 1979-1981, 1984-1985, 1987-1990 and 1997-1998. We can note that the negative phase 1982-1983 correspond to the dry years over this region. These components account for about 25.3% of the total variance. The PC2 of GPCP precipitation was in its negative phase between 1979-1997; while the PC3 of GPCP precipitation was in its positive phase in June to August and in its negative phase respectively between years 1980-1999 and 2002-2010. The PC2 and PC3 account respectively for around 20.5% and more than 14% of the total variance. The first corresponding three EOFs are presented in **Figure 9**. The EOF1 presents the permanent monsoon zone around the West Africa coast where the EOF2 shows this penetration in the continent and the Mountains areas convection.

4. Conclusion

Using upper air soundings, satellites, meteorological radar and instrumented aircrafts, convective activities over West African Sahel associated with the African monsoon have been documented extensively in recent years. Most recent research on the West African monsoon's intraseasonal variability (time scale of 10 to 90 days) has centered on the Madden-Julian Oscillation or MJO. In this work, we show that the maximum rainfall effectively occurs at mid August over West Africa where the maximum rainfall can be found in the West Africa coastal zone and particularly around the Fouta-Jalon Mountain. The trend of the precipitation presents a maximum at the center of Senegal in August, which corresponds to the presence of ICTZ in this region. We also found that the negative unfiltered OLR anomalies, composite structure of 850 hPa wind anomalies and precipitation anomalies are associated with African waves. Active phases are characterised by enhanced precipitation along 2.5°N. Enhanced trade winds accompany enhanced precipitation and convection. The 850-hPa wind and wind divergence structure show a maximum convection over Mountain region (Fouta-Djalou and Mont-Cameroon) which corresponds to the high precipitation and OLR observed in these regions.

The synoptic times-scales precipitation in West Africa during the summer 1980-2009 is dominated by variability on both 3 - 5 and 5 - 6 day times-scales. The 3-day peak is presumably in association with African easterly waves and with convective activity over land whereas the 5-day peak presumably corresponds to 5 - 6 days synoptic variability. Over the Northern Senegal (14°N - 16.5°N and 12°W - 16.5°W), the largest oscillations of convection are observed during June-August with synoptic variance between 2 and 5 days. It also shows the first three PC and EOF of GPCP precipitations over West Africa during the summer (JAS) from 1979 to 2010. The PC1 accounts for 25.3% of the total variance. The PC2 of GPCP precipitation was generally in its negative phase between

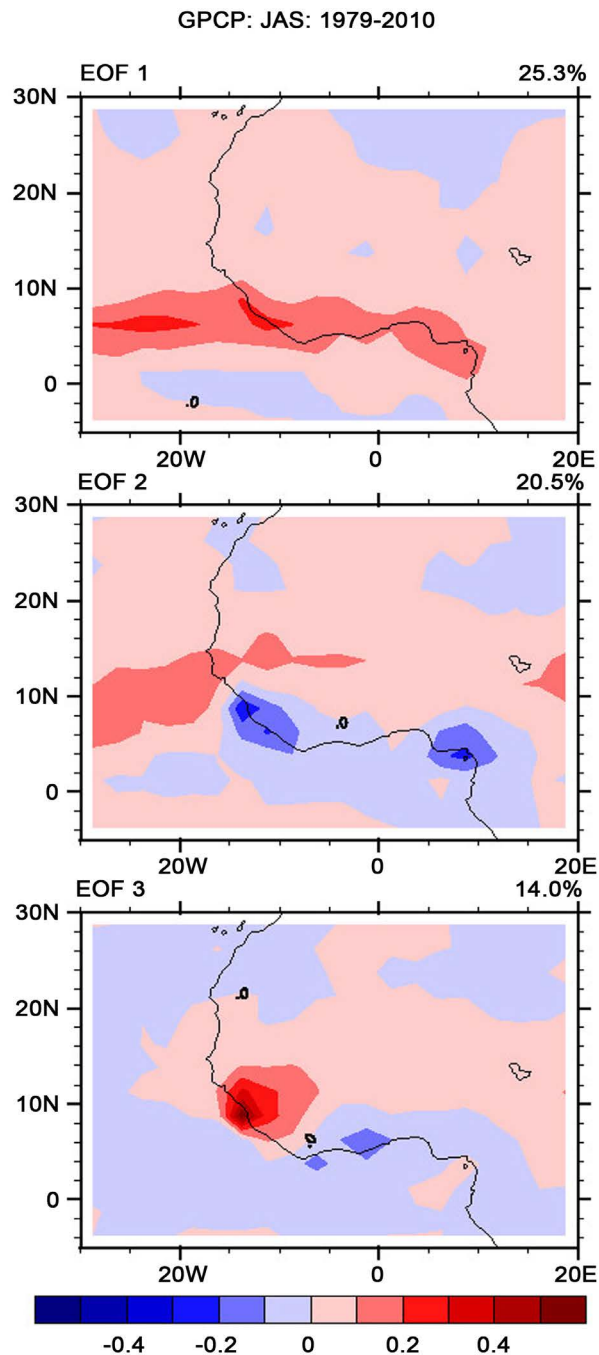


Figure 9. First three EOF of GPCP precipitation over West Africa during June - July-August - September 1979-2010. Percentage of total variance accounting for the pattern appears on top right corner.

1979-1997 while the PC3 of GPCP precipitation was in its positive phase in June and August and in its negative phase in July and September respectively between years 1980-1999 and 2002-2010. The PC2 and PC3 account respectively for around 20.5% and more than 14% of the total variance.

Future research over West Africa Sahel should focus on examining additional precipitation events in different developing and/or non-developing AEWs and

compare the data more directly to previous satellite-derived climatology (e.g. TRMM or Cloudsat products).

Acknowledgements

The authors thank the housed at the UFR of Applied Sciences and Technology (UFR SAT) of the Gaston Berger University (UGB) of Saint-Louis in Senegal (CEA-MITIC) for funding the stay in Douala of one of them (Dia-Diop A.). They are also grateful to the ECMWF for making their Era-Interim product available to them.

Conflicts of Interest

The authors declare no conflicts of interest regarding the publication of this paper.

References

- Boone, A., De Rosnay, P., Balsamo, G. et al. (2009). The AMMA Land Surface Model Intercomparison Project (ALMIP). *Bulletin of the American Meteorological Society*, *90*, 1865-1880. <https://doi.org/10.1175/2009BAMS2786.1>
- Daniell, P. J. (1946). Discussion on the Symposium on Autocorrelation in Time Series. *Journal of the Royal Statistical Society*, *8*, 88-90.
- Dee, D. P. et al. (2011). The ERA-Interim Reanalysis: Configuration and Performance of the Data Assimilation System. *Quarterly Journal of the Royal Meteorological Society*, *137*, 553-597. <https://doi.org/10.1002/qj.828>
- Diallo, I., Sylla, M. B., Giorgi, F., Gaye, A. T., & Camara, M. (2012). Multimodel GCM-RCM Ensemble Based Projections of Temperature and Precipitation over West Africa for the Early 21st Century. *International Journal of Geophysics*, *2012*, Article ID: 972896. <https://doi.org/10.1155/2012/972896>
- Dinku, T., Ceccato, P., Grover-Kopec, E., Lemma, M., Connor, S. J., & Ropelewski, C. F. (2007). Validation of Satellite Rainfall Products over East Africa's Complex Topography. *International Journal of Remote Sensing*, *28*, 1503-1526. <https://doi.org/10.1080/01431160600954688>
- Fontaine, B., & Janicot, S. (1992). Wind-Field Coherence and Its Variations over West Africa. *Journal of Climate*, *5*, 521-523. [https://doi.org/10.1175/1520-0442\(1992\)005<0512:WFCAIV>2.0.CO;2](https://doi.org/10.1175/1520-0442(1992)005<0512:WFCAIV>2.0.CO;2)
- Fontaine, B., Janicot, S., & Moron, V. (1995). Rainfall Anomaly Patterns and Wind Field Signals over West Africa in August (1958-1989). *Journal of Climate*, *8*, 1503-1510. [https://doi.org/10.1175/1520-0442\(1995\)008<1503:RAPAWF>2.0.CO;2](https://doi.org/10.1175/1520-0442(1995)008<1503:RAPAWF>2.0.CO;2)
- Giannini, A., Saravanan, R., & Chang, P. (2003). Oceanic Forcing of Sahel Rainfall on Interannual to Interdecadal Time Scales. *Science*, *302*, 1027-1030. <https://doi.org/10.1126/science.1089357>
- Gilman, D., Fuglister, P., & Mitchell, J. M. (1963). On the Power Spectrum of Red Noise. *Journal of the Atmospheric Sciences*, *20*, 1982-1984. [https://doi.org/10.1175/1520-0469\(1963\)020<0182:OTPSON>2.0.CO;2](https://doi.org/10.1175/1520-0469(1963)020<0182:OTPSON>2.0.CO;2)
- Hagos, S. M., & Cook, K. H. (2007). Dynamics of the West African Monsoon Jump. *Journal of Climate*, *20*, 5264-5284. <https://doi.org/10.1175/2007JCLI1533.1>
- Hoerling, M., Hurrell, J., Eischeid, J., & Phillips, A. (2006). Detection and Attribution of

- Twentieth-Century Northern and Southern African Rainfall Change. *Journal of Climate*, 19, 3989-4008. <https://doi.org/10.1175/JCLI3842.1>
- Janicot, S. (2011). Intra-Seasonal Variability of the West African Monsoon. *Atmospheric Science Letters*, 12, 24-30. <https://doi.org/10.1002/asl.280>
- Janicot, S., Mounier, F., & Diedhiou, A. (2008). Les ondes atmosphériques d'échelle synoptique dans la mousson d'Afrique de l'Ouest et centrale: Ondes d'est et onde de Kelvin. *Sécheresse*, 19, 13-22.
- Jenkins, G., Kucera, P., Joseph, E., Fuentes, J., Gaye, A., Gerlach, J., Roux, F., Viltard, N., Papazzoni, M., Protat, A., Bouniol, D., Reynolds, A., Arnault, J., Badiane, D., Kebe, F., Camara, M., Sall, S., Ndiaye, S. A., & Deme, A. (2010). Observations of Weather Features in Senegal during the AMMA SOP-3 Period. *Journal of Geophysical Research: Atmospheres*, 115, D18108. <https://doi.org/10.1029/2009JD013022>
- Kidson, J. W. (1977). African Rainfall and Its Relation to Upper Air Circulation. *Quarterly Journal of the Royal Meteorological Society*, 103, 441-456. <https://doi.org/10.1002/qj.49710343705>
- Kiladis, G. N., Wheeler, M. C., Haertel, P. T., Straub, K. H., & Roundy, P. E. (2009). Convectively Coupled Equatorial Waves. *Reviews of Geophysics*, 47, RG2003. <https://doi.org/10.1029/2008RG000266>
- Lamb, P. J. (1978). Case Studies of Tropical Atlantic Surface Circulation Patterns during Recent Sub-Saharan Weather Anomalies: 1967 and 1968. *Monthly Weather Review*, 106, 482-491. [https://doi.org/10.1175/1520-0493\(1978\)106<0482:CSOTAS>2.0.CO;2](https://doi.org/10.1175/1520-0493(1978)106<0482:CSOTAS>2.0.CO;2)
- Le Barbé, L., Lebel, T., & Tapsoba, D. (2002). Rainfall Variability in West Africa during the Years 1950-90. *Journal of Climate*, 15, 187-202. [https://doi.org/10.1175/1520-0442\(2002\)015<0187:RVIWAD>2.0.CO;2](https://doi.org/10.1175/1520-0442(2002)015<0187:RVIWAD>2.0.CO;2)
- Lebel, T., Cappelaere, B., Galle, S. et al. (2009). AMMA-CATCH Studies in the Sahelian Region of West-Africa: An Overview. *Journal of Hydrology*, 375, 3-13. <https://doi.org/10.1016/j.jhydrol.2009.03.020>
- Lenouo, A., Mkankam, K. F., & Yepdjuo, E. (2005). Weak Interaction in the African Easterly Jet. *Annales Geophysicae*, 23, 1637-1643. <https://doi.org/10.5194/angeo-23-1637-2005>
- Lenouo, A., Sall, M. S., Badiane, D., Gaye, A. T., & Mkankam, K. F. (2016). Intense Convection over West Africa during AMMA SOP3 Experiment. *Atmospheric Research*, 180, 1-11. <https://doi.org/10.1016/j.atmosres.2016.05.002>
- Liebmann, B., & Smith, C. A. (1996). Description of a Complete (Interpolated). Outgoing Longwave Radiation Dataset. *Bulletin of the American Meteorological Society*, 77, 1275-1277.
- McCollum, J., Nelkin, E., Klotter, D., Berte, Y., Diallo, B. M., Gaye, I., Kpabeba, G., Ndiaye, O., Noukpozoukhou, T. M. M., Thiam, A., Toure, A. A., Traore, K., Nicholson, S. E., & Some, B. (2003). Validation of TRMM and Other Rainfall Estimates with a High-Density Gauge Dataset for West Africa. Part I: Validation of GPCC Rainfall Product and Pre-TRMM Satellite and Blended Products. *Journal of Applied Meteorology*, 40, 1355-1368. [https://doi.org/10.1175/1520-0450\(2003\)042<1355:VOTAOR>2.0.CO;2](https://doi.org/10.1175/1520-0450(2003)042<1355:VOTAOR>2.0.CO;2)
- Ndao, S., Rinelle, D. N., Badiane, D., Lenouo, A., & Sall, S. M. (2019). Study of Boundary Layer Height over West Africa. *Journal of Geoscience and Environment Protection*, 7, 179-194. <https://doi.org/10.4236/gep.2019.711013>
- Newell, R. E., & Kidson, J. W. (1984). African Mean Wind Changes in Sahelian Wet and Dry Periods. *Journal of Climatology*, 4, 1-7. <https://doi.org/10.1002/joc.3370040103>
- Nguyen, T. T. H., & Duvel, J. P. (2008). Synoptic Wave Perturbations and Convective Systems over Equatorial Africa. *Journal of Climate*, 21, 6372-6388.

- <https://doi.org/10.1175/2008JCLI2409.1>
- Nicholson, S. E. (1981). Rainfall and Atmospheric Circulation during Drought Periods and Wetter Years in West Africa. *Monthly Weather Review*, *109*, 2191-2208. [https://doi.org/10.1175/1520-0493\(1981\)109<2191:RAACDD>2.0.CO;2](https://doi.org/10.1175/1520-0493(1981)109<2191:RAACDD>2.0.CO;2)
- Nicholson, S. E. (2008). The Intensity, Location and Structure of the Tropical Rainbelt over West Africa as Factors in Interannual Variability. *International Journal of Climatology*, *28*, 1775-1785. <https://doi.org/10.1002/joc.1507>
- Nicholson, S. E. (2013). The West African Sahel: A Review of Recent Studies on the Rainfall Regime and Its Interannual Variability. *Meteorology*, *2013*, Article ID: 453521. <https://doi.org/10.1155/2013/453521>
- Nicholson, S. E., & Grist, J. P. (2001). A Conceptual Model for Understanding Rainfall Variability in the West African Sahel on Interannual and Interdecadal Timescales. *International Journal of Climatology*, *21*, 1733-1757. <https://doi.org/10.1002/joc.648>
- Nicholson, S. E., & Webster, P. J. (2007). A Physical Basis for the Interannual Variability of Rainfall in the Sahel. *Quarterly Journal of the Royal Meteorological Society*, *133*, 2065-2084. <https://doi.org/10.1002/qj.104>
- Paeth, H., & Hense, A. (2004). SST versus Climate Change Signals in West African Rainfall: 20th-Century Variations and Future Projections. *Climatic Change*, *65*, 179-208. <https://doi.org/10.1023/B:CLIM.0000037508.88115.8a>
- Redelsperger, J. L., Thorncroft, C. D., Diedhiou, A., Lebel, T., Parker, D. J., & Polcher, J. (2006). African Monsoon Multidisciplinary Analysis: An International Research Project and Field Campaign. *Bulletin of the American Meteorological Society*, *87*, 1739-1746. <https://doi.org/10.1175/BAMS-87-12-1739>
- Reed, R. J., Norquist, D. C., & Recker, E. E. (1977). The Structure and Properties of African Wave Disturbances as Observed during Phase III of GATE. *Monthly Weather Review*, *105*, 317-333. [https://doi.org/10.1175/1520-0493\(1977\)105<0317:TSAPOA>2.0.CO;2](https://doi.org/10.1175/1520-0493(1977)105<0317:TSAPOA>2.0.CO;2)
- Roundy, P. E. (2008). Analysis of Convectively Coupled Kelvin Waves in the Indian Ocean MJO. *Journal of the Atmospheric Sciences*, *65*, 1342-1359. <https://doi.org/10.1175/2007JAS2345.1>
- Ruiz, F. et al. (2010). Validation of Satellite Rainfall Products over Colombia. *Journal of Applied Meteorology and Climatology*, *49*, 1004-1014. <https://doi.org/10.1175/2009JAMC2260.1>
- Salack, S., Klein, C., Giannini, A., Sarr, B., Worou, O. N., Belko, N., Bliefernicht, J., & Kunstmann, H. (2016). Global Warming Induced Hybrid Rainy Seasons in the Sahel. *Environmental Research Letters*, *11*, 10. <https://doi.org/10.1088/1748-9326/11/10/104008>
- Semazzi, H. F. M., & Sun, L. (1997). The Role of Orography in Determining the Sahelian Climate. *International Journal of Climatology*, *17*, 581-596. [https://doi.org/10.1002/\(SICI\)1097-0088\(199705\)17:6<581::AID-JOC134>3.0.CO;2-E](https://doi.org/10.1002/(SICI)1097-0088(199705)17:6<581::AID-JOC134>3.0.CO;2-E)
- Tchakoutio, S. A., Nzeukou, A. T., & Tchawoua, C. (2012). Intraseasonal Atmospheric Variability and Its Interannual Modulation in Central Africa. *Meteorology and Atmospheric Physics*, *117*, 167-179. <https://doi.org/10.1007/s00703-012-0196-6>
- Thomas, M., John, C. H. C., Alexander, G., & Nicolas, J. C. (2009). Temporal Precipitation Variability versus Altitude on a Tropical High Mountain: Observations and Mesoscale Atmospheric Modeling. *Quarterly Journal of the Royal Meteorological Society*, *135*, 1439-1455. <https://doi.org/10.1002/qj.461>
- Thorncroft, C. D., Parker, D. J., & Burton, R. R. (2003). The JET2000 Project—Aircraft

- Observations of the African Easterly Jet and African Easterly Waves. *Bulletin of the American Meteorological Society*, 84, 337-351. <https://doi.org/10.1175/BAMS-84-3-337>
- Torrence, C., & Compo, G. P. (1998). A Practical Guide to Wavelet Analysis. *Bulletin of the American Meteorological Society*, 79, 61-78. [https://doi.org/10.1175/1520-0477\(1998\)079<0061:APGTWA>2.0.CO;2](https://doi.org/10.1175/1520-0477(1998)079<0061:APGTWA>2.0.CO;2)
- Vondou, D. A., Nzeukou, A., Lenouo, A., & Mkankam, K. F. (2010). Seasonal Variations in the Diurnal Patterns of Convection in Cameroon-Nigeria and Their Neighbouring Areas. *Atmospheric Science Letters*, 11, 290-300. <https://doi.org/10.1002/asl.297>
- Wang, G., & Eltahir, E. A. B. (2000). The Role of Vegetation Dynamics in Enhancing the Low-Frequency Variability of the Sahel Rainfall. *Water Resources Research*, 36, 1013-1021. <https://doi.org/10.1029/1999WR900361>
- Wheeler, M. C., & Kiladis, G. N. (1999). Convectively Coupled Equatorial Waves: Analysis of Clouds and Temperature in the Wave-Number Frequency Domain. *Journal of the Atmospheric Sciences*, 56, 374-399. [https://doi.org/10.1175/1520-0469\(1999\)056<0374:CCEWAO>2.0.CO;2](https://doi.org/10.1175/1520-0469(1999)056<0374:CCEWAO>2.0.CO;2)
- Wilks, D. (2011). *Statistical Methods in the Atmospheric Sciences* (3rd ed., Vol. 100, pp. 704). New York: International Geophysics.
- Zebaze, S., Lenouo, A., Tchawoua, C., & Janicot. C. (2015). Synoptic Kelvin Type Perturbation Waves over Congo Basin over the Period 1979-2010. *Journal of Atmospheric and Solar-Terrestrial Physics*, 130-131, 43-56. <https://doi.org/10.1016/j.jastp.2015.04.015>
- Zebaze, S., Lenouo, A., Tchawoua, C., & Mkankam, K. F. (2017). Interaction between Moisture Transport and Kelvin Waves Events over Equatorial Africa through ERA-Interim. *Atmospheric Science Letters*, 18, 300-306. <https://doi.org/10.1002/asl.756>